

RESEARCH ARTICLE

Open Access

A novel prostaglandin I₂ agonist, ONO-1301, attenuates liver inflammation and suppresses fibrosis in non-alcoholic steatohepatitis model mice

Satoko Motegi¹, Atsunori Tsuchiya^{1*}, Takahiro Iwasawa¹, Takeki Sato¹, Masaru Kumagai¹, Kazuki Natsui¹, Shunsuke Nojiri¹, Masahiro Ogawa¹, Suguru Takeuchi¹, Yosiki Sakai², Shigeru Miyagawa², Yoshiki Sawa² and Shuji Terai^{1*}

Abstract

Background: ONO-1301 is a novel long-lasting prostaglandin (PG) I₂ mimetic with inhibitory activity on thromboxane (TX) A₂ synthase. This drug can also induce endogenous prostaglandin (PG)I₂ and PGE₂ levels. Furthermore, ONO-1301 acts as a cytokine inducer and can initiate tissue repair in a variety of diseases, such as pulmonary hypertension, pulmonary fibrosis, cardiac infarction, and obstructive nephropathy. In this study, our aim was to evaluate the effect of ONO-1301 on liver inflammation and fibrosis in a mouse model of non-alcoholic steatohepatitis (NASH).

Methods: The therapeutic effects of ONO-1301 against liver damage, fibrosis, and occurrence of liver tumors were evaluated using melanocortin 4 receptor-deficient (*Mcr4r*-KO) NASH model mice. The effects of ONO-1301 against macrophages, hepatic stellate cells, and endothelial cells were also evaluated in vitro.

Results: ONO-1301 ameliorated liver damage and fibrosis progression, was effective regardless of NASH status, and suppressed the occurrence of liver tumors in *Mcr4r*-KO NASH model mice. In the in vitro study, ONO-1301 suppressed LPS-induced inflammatory responses in cultured macrophages, suppressed hepatic stellate cell (HSC) activation, upregulated vascular endothelial growth factor (VEGF) expression in HSCs, and upregulated hepatocyte growth factor (HGF) and VEGF expression in endothelial cells.

Conclusions: The results of our study highlight the potential of ONO-1301 to reverse the progression and prevent the occurrence of liver tumors in NASH using in vivo and in vitro models. ONO-1301 is a multidirectional drug that can play a key role in various pathways and can be further analyzed for use as a new drug candidate against NASH.

Keywords: ONO-1301, Prostacyclin, Prostaglandin I₂, Prostaglandin E₂, Non-alcoholic steatohepatitis

* Correspondence: atsunori@med.niigata-u.ac.jp; terais@med.niigata-u.ac.jp

¹Division of Gastroenterology and Hepatology, Graduate School of Medical and Dental Sciences, Niigata University, 1-757, Asahimachi-dori, Chuo-ku, Niigata 951-8510, Japan

Full list of author information is available at the end of the article



© The Author(s). 2022 **Open Access** This article is licensed under a Creative Commons Attribution 4.0 International License, which permits use, sharing, adaptation, distribution and reproduction in any medium or format, as long as you give appropriate credit to the original author(s) and the source, provide a link to the Creative Commons licence, and indicate if changes were made. The images or other third party material in this article are included in the article's Creative Commons licence, unless indicated otherwise in a credit line to the material. If material is not included in the article's Creative Commons licence and your intended use is not permitted by statutory regulation or exceeds the permitted use, you will need to obtain permission directly from the copyright holder. To view a copy of this licence, visit <http://creativecommons.org/licenses/by/4.0/>.

30 Background

31 Non-alcoholic fatty liver disease (NAFLD) and non-
32 alcoholic steatohepatitis (NASH) are among the most
33 important causes of chronic liver disease and cirrhosis,
34 mainly in South America and the Middle East, followed
35 by the rest of Asia, the USA, and Europe. It has been es-
36 timated that the incidence of NAFLD and NASH will in-
37 crease in the coming decade. While the epidemiology
38 and demographic characteristics of NAFLD vary world-
39 wide and NAFLD and NASH are generally detected in
40 lean patients, most of the cases are related to lifestyle
41 and obesity [1–3]. The most important countermeasures
42 are the correction of lifestyle, if possible, from a younger
43 age. However, parallel development of new drugs that
44 prevent the progression of inflammation and fibrosis is
45 essential [4].

46 To evaluate the effects of cell therapy and drugs in
47 NASH, appropriate animal models that reflect symptoms
48 in humans, such as obesity, insulin resistance, and liver
49 steatosis, are needed.

50 Melanocortin 4 receptor-deficient (*Mc4r*-KO) mice are
51 ideal models for evaluating the effects of cell therapy
52 and drugs against NASH [5–7]. MC4R is expressed in
53 the hypothalamic nuclei and regulates food intake and
54 body weight; thus, *Mc4r*-KO mice cannot control their
55 appetite and exhibit symptoms such as obesity, insulin
56 resistance, and liver steatosis similar to those of NASH
57 in humans. When a high-fat diet (HFD) was started 8
58 weeks after birth, steatohepatitis with fibrosis and hepa-
59 tocellular carcinoma were detected around 28 weeks and
60 1 year after birth, respectively, in the mice [8, 9]. Using
61 this model, we had previously evaluated the anti-
62 inflammatory and anti-fibrosis effects of mesenchymal
63 stem cells and their exosomes, and the mechanisms of
64 NASH-related carcinogenesis [5–7]. Thus, this mouse
65 model is ideal for evaluating the effects of drugs against
66 steatosis, fibrosis, and carcinogenesis.

67 ONO-1301 is a unique novel long-lasting prostaglan-
68 din (PG) I₂ mimetic with inhibitory activity on thromb-
69 oxane (TX) A₂ synthase. This drug is chemically and
70 biologically stable because of the lack of a typical prosta-
71 noid [10–18]. ONO-1301 acts primarily as a prostacyclin
72 receptor (IP) agonist and can induce adenosine cyclic
73 3',5'-monophosphate (cAMP) elevation in target cells.
74 However, IP agonists, when administered alone, usually
75 lose their efficacy after repeated administration. Further-
76 more, they increase TXA₂ production, which usually in-
77 creases blood pressure and thrombosis formation.
78 However, due to the inhibitory activity of ONO-1301 on
79 TXA₂ synthase, tolerance development caused by re-
80 peated administration of this IP agonist is suppressed
81 [19]. In addition, this drug can induce endogenous PGI₂;
82 PGE₂; and endogenous regenerative factors such as hep-
83 atocyte growth factor (HGF), vascular endothelial

growth factor (VEGF), and stromal cell derived factor 84
(SDF)-1, which induce tissue repair processes such as 85
angiogenesis, anti-fibrosis, anti-apoptosis, and nitric 86
oxide (NO) generation [10, 11, 13, 14]. Based on a few 87
reports, we suspected that ONO-1301 would have posi- 88
tive effects on acute liver injury. Yin et al. reported a 89
protective role of COX-2 derived PGs in concanavalin A 90
(ConA)-induced liver injury. In this study, COX-2^{-/-} 91
mice developed severe damage in the liver, and these ef- 92
fects were canceled by the PGE_{1/2} analog or the PGI₂ 93
analog [20]. Mayoral et al. also reported that COX-2 94
dependent PGs exert a protective effect against 95
lipopolysaccharide-induced injury in D-galactosamine- 96
preconditioned mice (LPS/D-DalN) and ConA-induced 97
acute liver injury model by an antiapoptotic/antinecrotic 98
effect by accelerating early hepatocyte proliferation [21]. 99
Indeed, Xu et al. reported that ONO-1301 decreased 100
serum AST and ALT levels, apoptotic liver cell numbers, 101
and expansion of necrotic areas in liver tissues. These 102
authors focused on ONO-1301-induced HGF and 103
showed that neutralization of endogenous HGF could 104
reverse the therapeutic effects of ONO-1301 [10]. 105

106 In this study, we evaluated the therapeutic effects and
107 mechanisms of action of ONO-1301 against NASH in
108 *Mc4r*-KO mice.

109 Methods

110 Mice

111 *Mc4r*-KO mice with a C57BL/6J background, which
112 were provided by Joel K. Elmquist (University of Texas
113 Southern Medical Center, Dallas, TX, USA), were used
114 to develop NASH model mice. The mice were fed a nor-
115 mal diet for 8 weeks (ND; CE-2; CLEA Japan, Inc.
116 Tokyo, Japan) and then a Western diet (WD; Research
117 Diets, Inc., New Brunswick, NJ, USA). Typically, after
118 20 weeks of continuous intake of WD, the liver shows
119 inflammation and fibrosis similar to that in human
120 NASH. To obtain macrophages and stellate cells,
121 C57BL/6 mice purchased from Charles River (Yoko-
122 hama, Japan) were used. All animals were housed in a
123 specific pathogen-free environment and maintained
124 under standard conditions with a 12-h day/night cycle
125 and access to food and water ad libitum. All animal ex-
126 periments were conducted in compliance with the regu-
127 lations and approval of the Institutional Animal Care
128 Committee of Niigata University.

129 ONO-1301

130 ONO-1301 (powder, H5001) was provided by Lind
131 Pharma Inc. (Osaka, Japan). For in vitro experiments,
132 ONO-1301 was dissolved in dimethyl sulfoxide (DMSO,
133 Nacalai Tesque Inc., Kyoto, Japan) to obtain a final con-
134 centration of 0.01–0.1 μM. To examine its in vivo effect,
135 ONO-1301 powder was mixed with WD at a 0.01%

136 weight ratio. The ONO-1301 concentration was measured using the plasma of *Mc4r*-KO mice that were administered ONO-1301 at 0.01% w/w for 20 weeks, and the mass of the liquid chromatograph was used to evaluate ONO-1301 concentration. The plasma concentration of ONO-1301 was 19.3 ± 6.1 ng/mL (means \pm standard error of measurement), which was within expected range.

[Q1] 144 Macrophage culture and assay

145 Bone marrow cells collected from the femurs of 10–12-week-old C57BL/6 male mice were cultured at 37 °C in the presence of 5% CO₂ in ultra-low attachment flasks (Corning Inc., Corning, NY, USA) in Dulbecco's modified Eagle's medium (DMEM)/F12 (Thermo Fisher Scientific, Waltham, MA, USA) containing 20 ng/mL macrophage colony stimulating factor-1 (Peprotech Inc., Rocky Hill, NJ, USA); the medium was changed twice weekly, as described previously [22, 23]. After 7 days, the collected macrophages were harvested and seeded in 6-well Nunc™ Cell-Culture Treated Multidishes (Thermo Fisher Scientific) at a density of 3×10^5 cells/well. Then, 25 ng/mL lipopolysaccharide (LPS from *Escherichia coli* O111:B4; catalog number L2630; Sigma-Aldrich, Tokyo, Japan) and 0.01 μM ONO-1301 or DMSO (control group) were added to the cultured macrophages. After 18 h, the macrophages were harvested, and the mRNA expression levels of genes encoding pro-inflammatory factors (e.g., interleukin-6 [*Il6*], tumor necrosis factor [*Tnf-a*], monocyte chemoattractant protein-1 [*Mcp-1*], and inducible nitric oxide synthase [*Inos*]) and anti-inflammatory factors (e.g., interleukin-10 [*Il10*], chitinase 3-like 3 [*Ym-1*], and macrophage mannose receptor [*Cd206*]) were evaluated using real-time polymerase chain reaction (PCR) (Supplementary Table 1).

170 Hepatic stellate cell culture and assay

171 Hepatic stellate cells (HSCs) were isolated from 35 ± 5-week-old C57BL/6 female mice. Briefly, to obtain the HSCs, the livers were digested with liver perfusion medium (Thermo Fisher Scientific) and liver digestive medium (Thermo Fisher Scientific). Non-parenchymal cells from the digested cells were fractionated using 11% HistoDenz (Sigma-Aldrich, St. Louis, MO, USA) at 2500 rpm for 20 min. After isolation, mouse HSCs were cultured on collagen type I-coated 12-well plates (AGC Techno Glass Co., Ltd., Haibara, Japan) in DMEM (Thermo Fisher Scientific) supplemented with 10% fetal bovine serum (FBS; Thermo Fisher Scientific), non-essential amino acid solution (Thermo Fisher Scientific), and penicillin-streptomycin-glutamine (Thermo Fisher Scientific). After 6 h of culture, cells were washed with PBS, the medium was changed, and ONO-1301 (0.1 μM) or DMSO (control group) was added to each well. The

medium was changed 24 h later. After 72 h, HSCs were harvested, and the mRNA expression levels of genes encoding activated HSC factors (α -smooth muscle actin [*Acta2*], type I collagen alpha 1 [*Col1a1*], type III collagen alpha 1 [*Col3a1*]), and quiescent HSC factors (cytoglobin [*Ctgb*] and Hedgehog interacting protein [*Hhip*]) were evaluated using real-time PCR (Supplementary Table 1).

Endothelial cell culture and assay

Human umbilical vein vascular endothelial cells (HUVECs) obtained from Promocell (Heidelberg, Germany) were cultured according to the manufacturer's instructions. Cells at passages 4–6 were used for all the experiments. ONO-1301 (0.1 μM) or DMSO (control group) was added to the cultured HUVECs. The medium was replaced 24 h later with fresh media containing ONO-1301 or DMSO. After 72 h, HUVECs were harvested, and the mRNA expression levels of stromal cell-derived factor-1 α [*Sdf1*], hepatocyte growth factor [*Hgf*], and vascular endothelial growth factor [*Vegf*] were evaluated using real-time PCR (Supplementary Table 1).

Real-time PCR

Total RNA was extracted using the RNeasy kit (Qiagen, Venlo, the Netherlands) and was reverse transcribed using a QuantiTect reverse transcription kit (Qiagen) according to the manufacturer's instructions. Gene expression analysis was performed using pre-validated QuantiTect primers (Supplementary Table 1) with the QuantiTect SYBR reagent (Qiagen). Real-time PCR was performed using the Step One Plus Real-time PCR System (Applied Biosystems, Foster City, CA, USA). Results were obtained from five to seven replicates. The gene encoding glyceraldehyde 3-phosphate dehydrogenase (*Gapdh*) was used as an internal control (Supplementary Table 1). The fold change in relative gene expression compared to the control was calculated using the $\Delta\Delta Ct$ method.

Serum analyses

Blood samples were obtained from the hearts of mice at 20 and 28 weeks after starting WD feeding. Mice were anesthetized, and blood was collected by cardiac puncture for biochemical analyses in the non-fasted state. Serum alanine aminotransferase (ALT), aspartate transaminase (AST), total bilirubin (Bil), albumin (ALB), total triglyceride (TG), and total cholesterol (T-cho) levels were calculated by Oriental Yeast Co., Ltd. (Tokyo, Japan).

Immunohistochemistry

For staining of the liver tissue, 10% formalin-fixed tissue was sliced into 4-μm-thick sections. Immunohistochemistry

238 for F4/80 (ab111101; rabbit monoclonal to F4/80, dilution
239 1/80; Abcam, Cambridge, UK) was performed as follows.
240 The dewaxed tissues were subjected to antigen retrieval in
241 10 mM sodium citrate buffer (pH 6.0) for 20 min using a
242 microwave. Endogenous peroxidase activity was blocked by
243 treatment with 3% hydrogen peroxide (H₂O₂; FUJIFILM
244 Wako Pure Chemical Corporation, Osaka, Japan) in PBS
245 for 10 min at room temperature, followed by avidin-biotin
246 blocking. The primary antibody was applied overnight in an
247 antibody diluent reagent solution (Thermo Fisher Sci-
248 entific). The secondary antibody reaction was per-
249 formed using the Vecstain ABC kit (Vector
250 Laboratories, Burlingame, CA, USA). The sections
251 were stained by reaction with DAB TRIS tablets (Muto
252 Pure Chemicals, Tokyo, Japan). The number of hepatic
253 crown-like structures (hCLS) and histological features
254 of macrophages in the liver from NASH were counted
255 in at least 10 fields at × 200 magnification of each F4/
256 80-stained section and expressed as the mean num-
257 ber/mm².

258 Sirius Red staining

259 To quantify fibrosis, liver tissues were collected at 20
260 and 28 weeks after the start of WD feeding. Tissues were
261 fixed with 10% formalin, sliced into 4-μm-thick sections,
262 and stained with Sirius Red. The images of each section
263 were randomly (20 fields at × 200 magnification/mouse)
264 captured using a BZ-9000 microscope (Keyence, Osaka,
265 Japan), and quantitative analysis of the fibrotic area was
266 performed using the ImageJ software (version 1.6.0 20,
267 National Institutes of Health, Bethesda, MD, USA).

268 Hydroxyproline assay

269 The levels of hydroxyproline, which is a representative
270 collagen component, were determined in mouse livers at
271 20 and 28 weeks after starting WD feeding. Briefly, liver
272 samples (20 mg) were homogenized and subjected to
273 QuickZyme hydroxyproline assays (QuickZyme Bio-
274 science, Zernikedreef, the Netherlands) according to the
275 manufacturer's protocol. Liver tissue samples were ex-
276 tracted, and the absorbance was measured at 570 nm.
277 Data are expressed as the amount of hydroxyproline per
278 mg liver tissue.

279 Measurement of cAMP accumulation

280 cAMP was quantified from liver homogenates using a
281 Direct cAMP ELISA Kit (ab133051; Abcam, Cambridge,
282 UK) according to the manufacturer's protocol and
283 normalized to total liver weight. Intracellular cAMP
284 concentration of cultured macrophages and HUVECs
285 was quantified 30 min after the start of stimulation
286 using the Direct cAMP ELISA Kit (Enzo Life Sci-
287 ences, Farmingdale, NY, USA) according to the man-
288 ufacturer's protocol.

Statistical analysis

289 Statistical analysis was performed using GraphPad
290 Prism9 software (GraphPad Software Inc., La Jolla, CA,
291 USA). Data are presented as means ± standard deviation
292 (SD). The results were assessed using Welch's *t*-test. Dif-
293 ferences between groups were analyzed using Welch's
294 one-way analysis of variance (ANOVA). Differences were
295 considered significant at $p < 0.05$.
296

Results

297 ONO-1301 ameliorates liver damage and fibrosis 298 progression in NASH model mice

299 To evaluate the therapeutic effects of ONO-1301, it was
300 mixed into mice feed and administered to *Mc4r*-KO
301 NASH model mice from 8 weeks after birth (ONO
302 group). Serum biochemical levels and fibrosis accumula-
303 tion were evaluated in comparison with the levels in the
304 WD feeding control group (Ctl group) (Fig. 1a).
305

306 Analyses of serum biochemical parameters and liver-
307 to-body weight ratio revealed that serum levels of ALT
308 (Ctl group: 410 ± 136.8 IU/L, ONO group: 226.3 ± 82.7
309 IU/L, $p = 0.0020$), ALP (Ctl group: 643.4 ± 190.5 IU/L,
310 ONO group: 333.7 ± 135.5 IU/L, $p = 0.0005$), T-cho (Ctl
311 group: 335.7 ± 33.9 mg/dL, ONO group: 274.8 ± 47.1
312 mg/dL, $p = 0.0021$), and the liver-to-body weight ratio
313 (Ctl group: 10.17 ± 1.46 g, ONO group: 8.63 ± 1.16 g, p
314 = 0.0126) were significantly lower in the ONO-1301
315 feeding group compared to those in the control group
316 (Fig. 1b). Evaluation of fibrosis demonstrated that the
317 Sirius Red stained area (Ctl group: 3.10% ± 2.59%, ONO
318 group: 1.12% ± 1.01%, $p < 0.0001$; Fig. 1c) and hydroxy-
319 proline levels (Ctl group: 5.61 ± 1.15 nmol/mg, ONO
320 group: 4.71 ± 0.86 nmol/mg, $p = 0.0008$; Fig. 1d) were
321 significantly decreased in the ONO-1301 feeding group
322 compared to those in the control group. Moreover,
323 ONO-1301 significantly reduced the number of hCLS,
324 indicating that the macrophages aggregated around hep-
325 atocytes with large lipid droplets in the liver (Fig. 1e).
326 In addition, we confirmed that cAMP levels in the liver
327 tissues were tended to increase after ONO-1301 treat-
328 ment (Fig. 1f). These results revealed that oral adminis-
329 tration of ONO-1301 effectively ameliorated liver
330 damage and fibrosis.

331 ONO-1301 was effective regardless of status of NASH and 332 suppressed liver tumor formation

333 Next, to evaluate whether the therapeutic effect of
334 ONO-1301 varied depending on the status of NASH, we
335 divided the mice into three groups as follows: In the Ctl
336 group, the *Mc4r*-KO mouse fed ND until 8 weeks, fol-
337 lowing which WD was fed until 28 weeks after birth. In
338 the Mid-ONO group, mice fed ND until 8 weeks after
339 birth were then fed WD for 20 weeks, followed by WD
340 with ONO-1301 for 8 weeks under conditions similar to

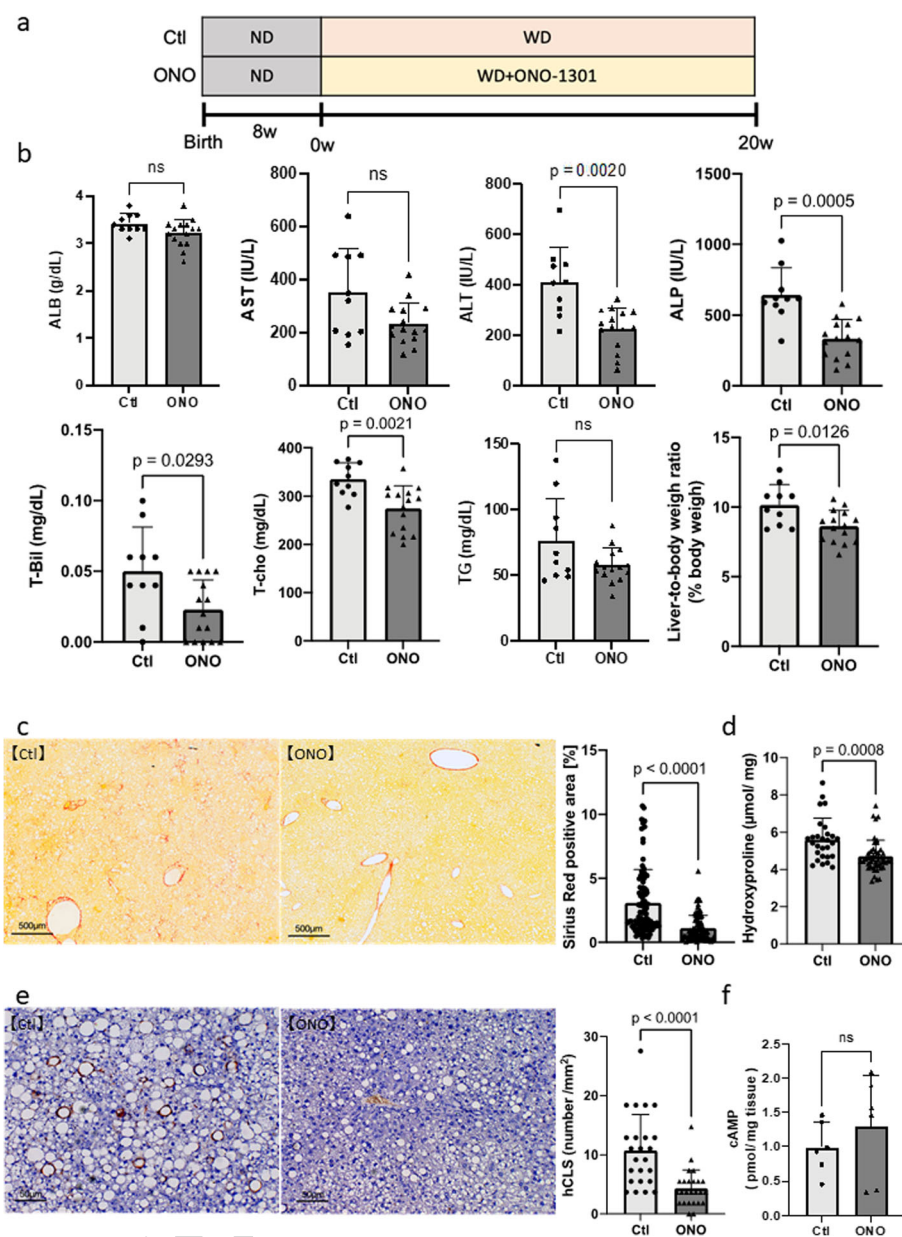


Fig. 1 Therapeutic effects of ONO-1301 (20 weeks of treatment) in the *Mc4r*-KO NASH model mice. *Mc4r*-KO mice were fed a Western diet from 8 weeks of age and followed up for an additional 20 weeks. **A** Schematic of the experiment. **B** Serum levels of albumin (ALB), aspartate transaminase (AST), alanine transaminase (ALT), alkaline phosphatase (ALP), total bilirubin (T-Bil), total cholesterol (T-cho), and triglyceride (TG). Liver-to-body weight ratios were analyzed. **C** Sirius Red staining of liver tissues. Scale bar = 500 μm. The quantification of Sirius Red staining. **D** Quantification of hydroxyproline. **E** Immunohistochemistry of F4/80 and quantification of hepatic crown-like structures (hCLS). **F** The levels of cAMP in the liver tissues. Scale bar = 50 μm. Total number of mice in each group: *n* = 6–10 in Ctl group, *n* = 6–15 in ONO group. Data are presented as mean ± standard deviation. ns: not significant

f1.1 those of the Ctl group. In the Long-ONO group, mice
 f1.2 fed ND until 8 weeks after birth, followed by WD with
 f1.3 ONO-1301 for 28 weeks (Fig. 2a).
 Q2 f1.4 While serum levels of ALB, AST, T-cho, and TG did
 f1.5 not change significantly in the mid-ONO group com-
 f1.6 pared to those in Ctl group, serum levels of ALT (Ctl
 f1.7 group: 397.8 ± 118.3 IU/L, mid-ONO group: 234.5 ±
 f1.8

95.7 IU/L, *p* = 0.0052) and ALP (Ctl group: 626.9 ± 348
 219.6 IU/L, mid-ONO group: 367.1 ± 116.0 IU/L, *p* = 349
 0.0061) and the liver-to-body weight ratio (Ctl group: 350
 11.12 ± 1.41 g, mid-ONO group: 9.64 ± 1.38 g, *p* = 351
 0.0399) in the mid-ONO group were decreased com- 352
 pared to those in the control group (Fig. 2b). These re- 353
 sults revealed that ONO-1301 is effective against 354

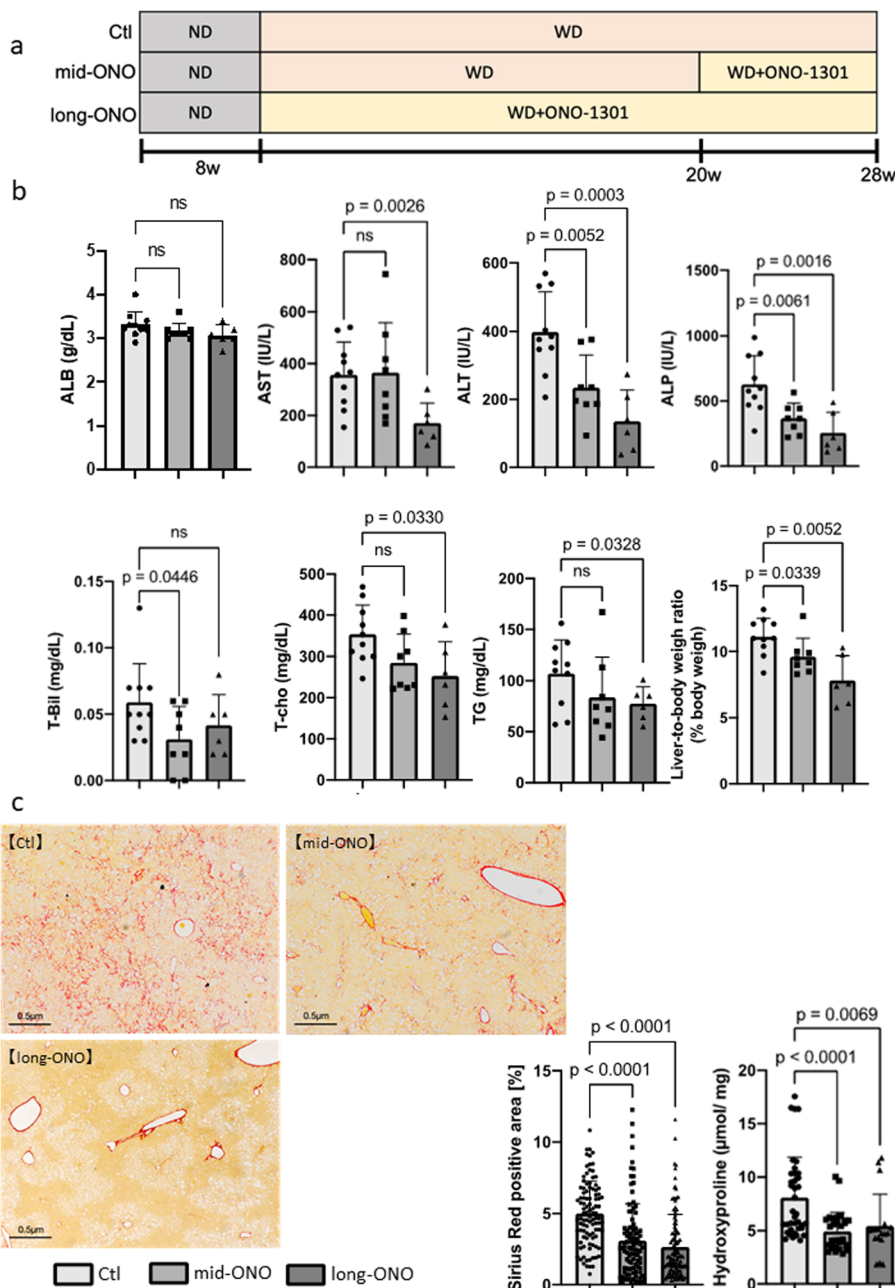


Fig. 2 Therapeutic effects of ONO-1301 (8- or 28-week treatment) in *Mc4r*-KO NASH model mice. *Mc4r*-KO mice were fed a Western diet from 8 weeks of age and followed up for an additional 28 weeks. **A** Schematic of the experiment. **B** Serum levels of albumin (ALB), aspartate transaminase (AST), alanine transaminase (ALT), alkaline phosphatase (ALP), total bilirubin (T-Bil), total cholesterol (T-cho), and triglyceride (TG). Liver-to-body weight ratios were analyzed. **C** Sirius Red staining and **D** quantification of hydroxyproline levels. Total number of mice in each group: *n* = 10 in Ctl group, *n* = 8 in mid-ONO group, *n* = 6 in long-ONO group. Scale bar = 500 µm. Data are presented as mean ± standard deviation. ns: not significant

355 established NASH. Furthermore, analyses of serum bio-
 356 chemical parameters and liver-to-body weight ratio re-
 357 vealed that serum levels of AST (Ctl group: 356.7 ± 126.7
 358 IU/L; long-ONO group: 171.2 ± 76.5 IU/L, *p* = 0.0026),
 359 ALT (Ctl group: 397.8 ± 118.3 IU/L, long-ONO group:
 360 135.8 ± 91.5 IU/L, *p* = 0.0003), ALP (Ctl group: 626.9 ±

219.6 IU/L, long-ONO group: 256.0 ± 156.6 IU/L, *p* =
 0.0016), T-cho (Ctl group: 353.8 ± 71.0 IU/L, long-ONO
 group: 253.2 ± 82.1 IU/L, *p* = 0.033), and TG (Ctl group:
 107.0 ± 32.9 IU/L, long-ONO group: 77.5 ± 16.6 IU/L, *p* =
 0.0328), and liver-to-body weight ratio (Ctl group: 11.12 ±
 1.41 g, long-ONO group: 7.83 ± 1.86 g, *p* = 0.005) in the

367 long-ONO group decreased significantly compared to
 368 those in the Ctl group (Fig. 2b). These results con-
 369 firmed the sustainable effects of ONO-1301 and that
 370 the long-term use of ONO-1301 improved lipid-
 371 related markers.

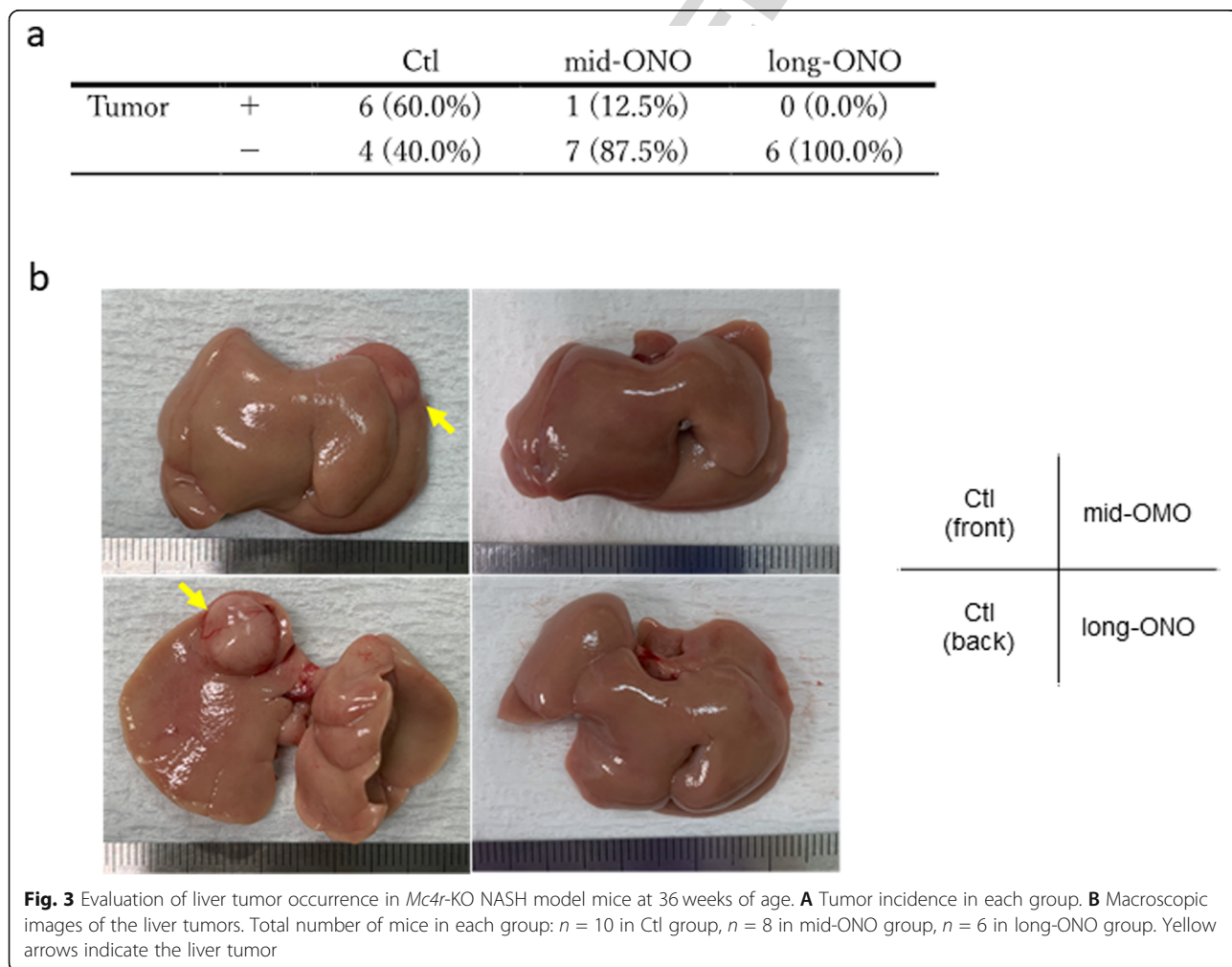
372 Evaluation of fibrosis demonstrated that the Sirius
 373 Red-stained area (Ctl group: 5.03% ± 2.21%, mid-ONO
 374 group: 3.09% ± 2.59% $p < 0.0001$, long-ONO group;
 375 2.65% ± 2.27% $p < 0.0001$; Fig. 2c) and hydroxyproline
 376 levels (Ctl group: 8.08 ± 3.79 nmol/mg, mid-ONO group:
 377 4.94 ± 1.79 nmol/mg, $p = 0.0001$; long-ONO group; 5.45
 378 ± 2.94 nmol/mg $p = 0.0069$; Fig. 2d) were significantly
 379 reduced in the ONO-1301 feeding group compared to
 380 those in the control group. Finally, we evaluated the oc-
 381 currence of liver tumors in the three groups and found
 382 that it was suppressed depending on the period of use of
 383 ONO-1301 (Ctl group: 6/10, 60.0 %; mid-ONO group,
 384 1/8 12.5 %; long-ONO group, 0/6 0.0%) (Fig. 3a, b).
 385 These results suggested that ONO-1301 was effective re-
 386 gardless of NASH status and suppressed the occurrence
 387 of liver tumors.

ONO-1301 suppressed LPS-induced inflammatory responses in cultured macrophages

388
 389 Macrophages have polarity and are key players in both pro-
 390 inflammatory and anti-inflammatory responses [24, 25].
 391 LPS, a component of gram-negative bacteria, is known to in-
 392 duce pro-inflammatory effects in macrophages by upregulat-
 393 ing the expression levels of *Il6*, *Mcp1*, *Tnfa*, and *Inos* in
 394 macrophages isolated from the bone marrow of WT mice.
 395 To confirm whether ONO-1301 can suppress pro-
 396 inflammatory effects in macrophages, ONO-1301 was added
 397 to macrophage cultures with or without LPS (Fig. 4a). LPS
 398 can upregulate the mRNA of pro-inflammatory markers *Il6*,
 399 *Mcp1*, *Tnfa*, and *Inos*. ONO-1301 significantly suppressed
 400 the LPS-induced pro-inflammatory markers *Mcp1*, *Tnfa*,
 401 and *Inos*. However, in the presence or absence of LPS,
 402 ONO-1301 did not affect mRNA expression levels of the
 403 anti-inflammatory macrophage markers *Il10* and *Cd206*
 404 (Fig. 4b). We also checked the cAMP levels of macrophages
 405 after adding ONO-1301 and confirmed that cAMP levels
 406 were significantly elevated after addition of ONO-1301 (Fig.
 407 4c). These results revealed that ONO-1301 suppressed the
 408

F3

F4



f3.1
 f3.2
 f3.3
 f3.4

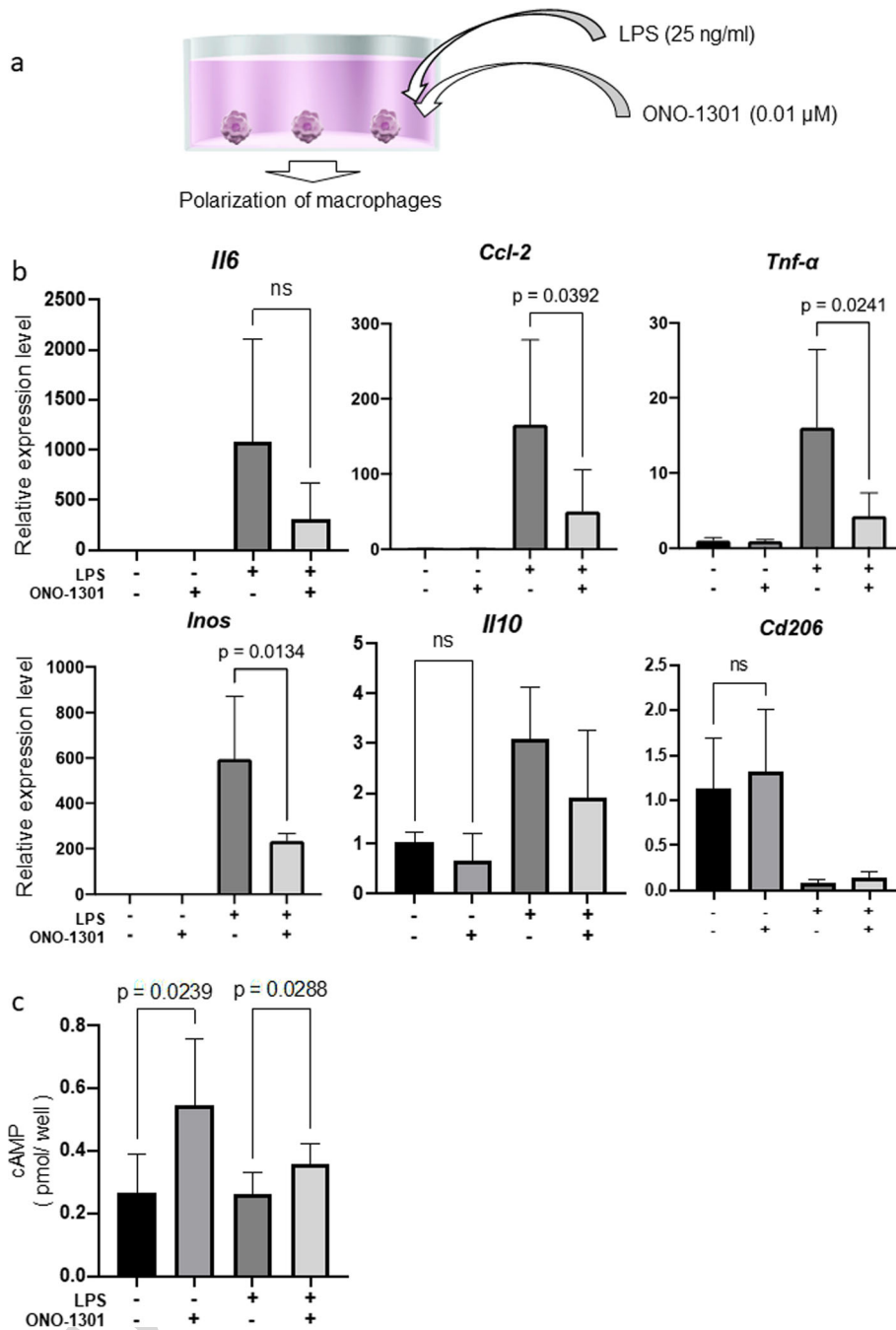


Fig. 4 Effects of ONO-1301 against macrophages in vitro. **A** Schematic of the experiment. **B** After addition of lipopolysaccharide (25 ng/ml), ONO-1301 (0.01 μM) to macrophage cultures, mRNA expression levels of *Il6*, *Ccl2*, *Tnf-α*, *Inos*, *Il10*, and *Cd206* were analyzed (each experiment was repeated seven times). **C** cAMP levels of each condition were analyzed of three independent experiments. Data are presented as mean ± standard deviation. ns: not significant

409 inflammatory response of cultured macrophages as IP
410 agonist.

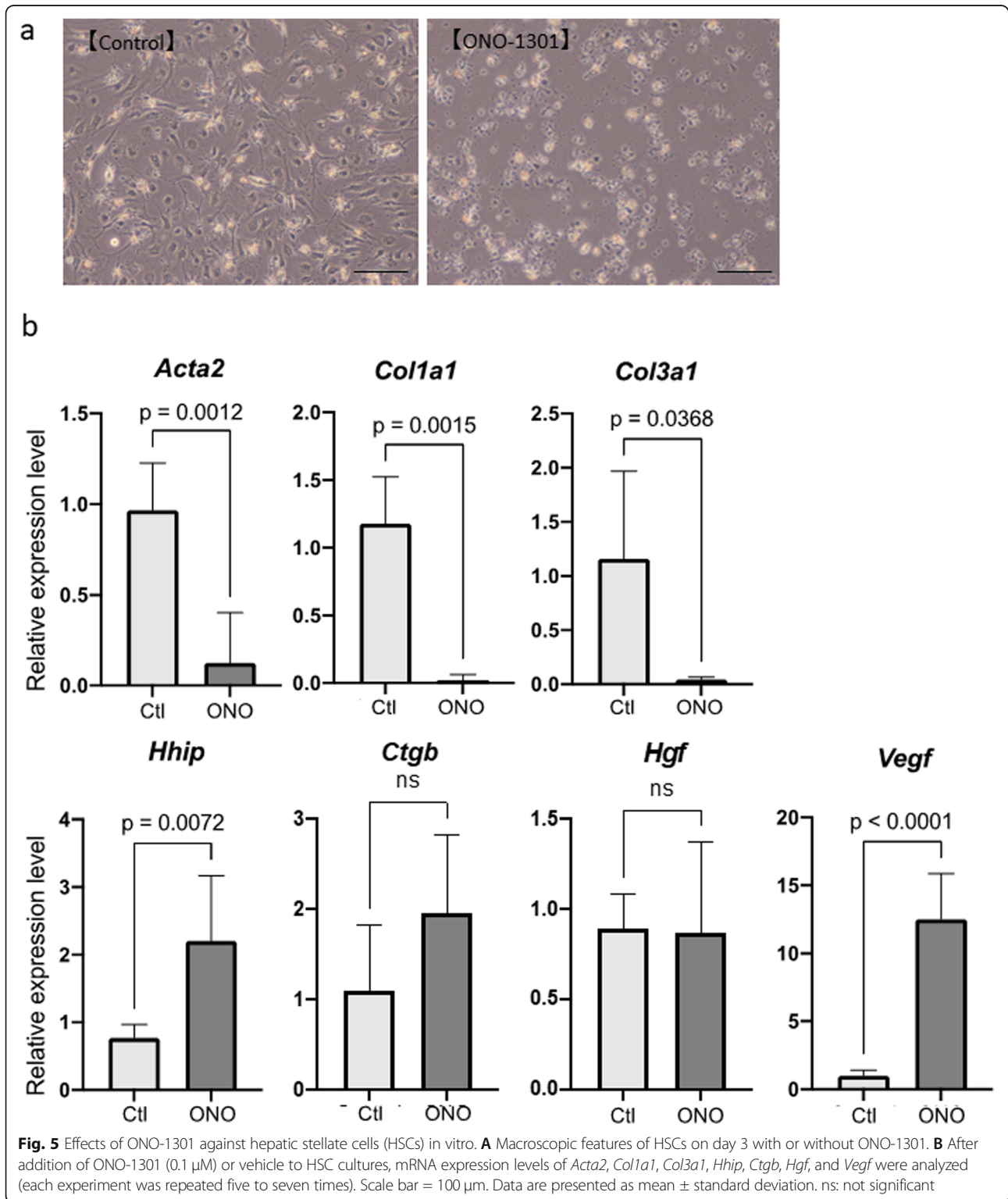
411 **ONO-1301 suppressed HSC activation and upregulated**
412 **VEGF expression**

413 HSCs are a major source of collagen fibers. Usually, har-
414 vested quiescent HSCs are activated when cultured on

collagen-coated dishes. During this activation, HSCs 415
produce collagen fibers and contribute to the formation 416
of fibrosis [24, 25]. To determine whether ONO-1301 417
directly inhibits HSC activation, mouse HSCs were har- 418
vested and seeded on collagen-coated dishes, and after 6 419
h, ONO-1301 was either added (ONO group) or not 420
(Ctl group). After 72 h of addition, the mRNA levels of 421

422 *Acta2*, *Col1a1*, *Col3a1*, *Ctgb*, *Hhip*, *Vegf*, and *Hgf* were
 423 assessed using real-time PCR. Macroscopically, while
 424 spinous processes, which suggest the activation of HSCs,
 425 were detected in the Ctl group, these processes were not
 F5 426 noticeable in the ONO group (Fig. 5a). mRNA levels of

activated HSC markers *Acta2*, *Col1a1*, and *Col3a1* were 427
 significantly suppressed after the addition of ONO-1301, 428
 and the mRNA levels of the quiescent HSC marker *Hhip* 429
 were significantly higher than those in the Ctl groups 430
 (Fig. 5b). Furthermore, the expression of *Vegf* was 431



f5.1
 f5.2
 f5.3
 f5.4

432 significantly upregulated in the ONO group compared
 433 to that in the Ctl group. We could not calculate the
 434 cAMP levels due to the shortage of cells obtained from
 435 primary culture. These results revealed that ONO-1301
 436 suppressed HSC activation and upregulated VEGF
 437 expression.

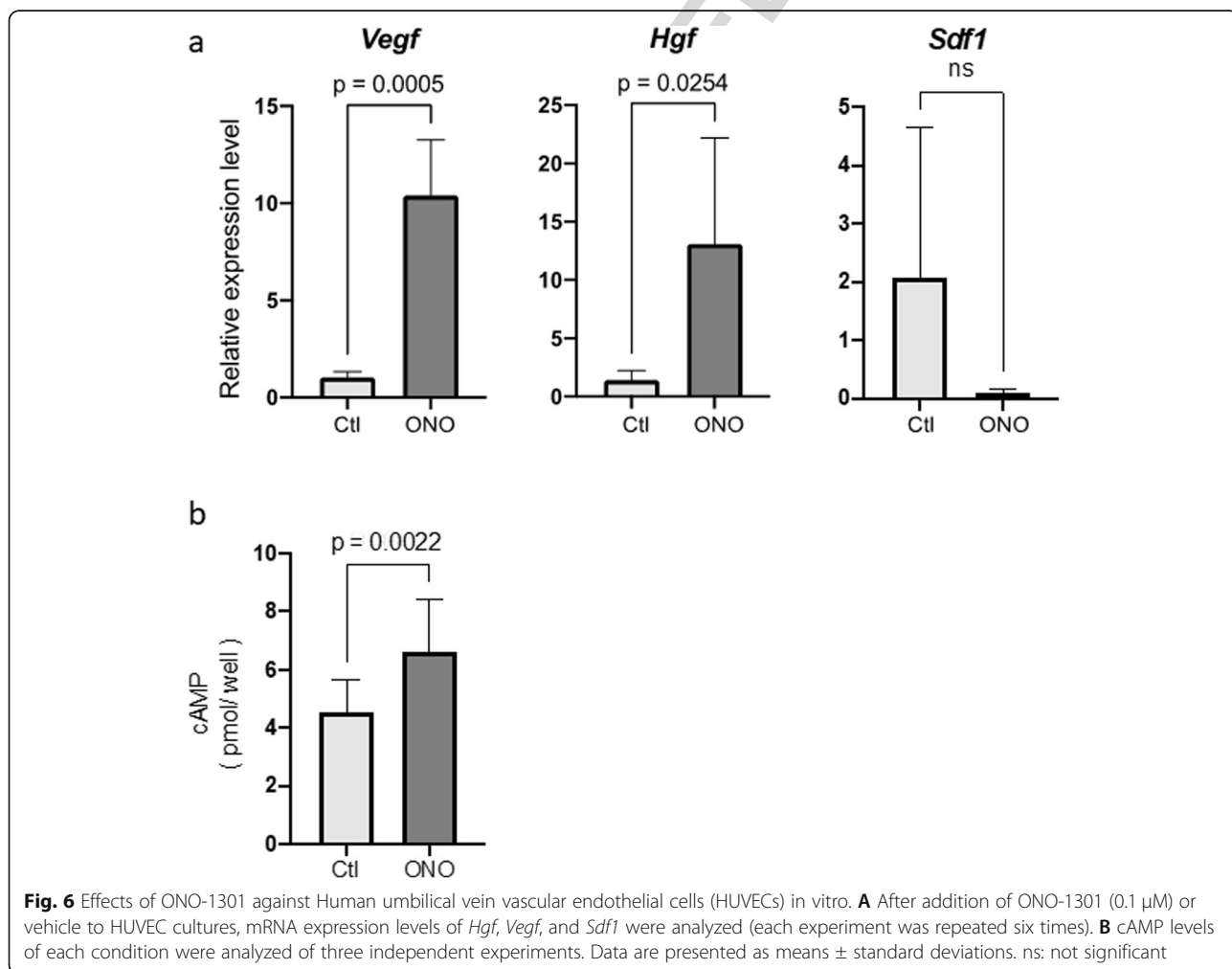
438 **ONO-1301 upregulates Hgf and Vegf expression in**
 439 **endothelial cells**

440 Finally, we examined the effects of ONO-1301 on hu-
 441 man umbilical vein endothelial cells (HUVECs).
 442 HUVECs were cultured in 6-well plates in the absence
 443 (Ctl group) or in the presence of ONO-1301 (ONO
 444 group). After culturing the HUVECs for 72 h, *Hgf*, *Vegf*,
 445 and *Sdf1* mRNA levels were assessed using real-time
 446 PCR. ONO-1301 increased the mRNA expression of *Hgf*
 447 and *Vegf* but did not affect the mRNA expression of
F6 448 *Sdf1* (Fig. 6a). We also checked the cAMP levels of
 449 HUVECs after adding ONO-1301 and confirmed that
 450 cAMP levels were significantly elevated after addition

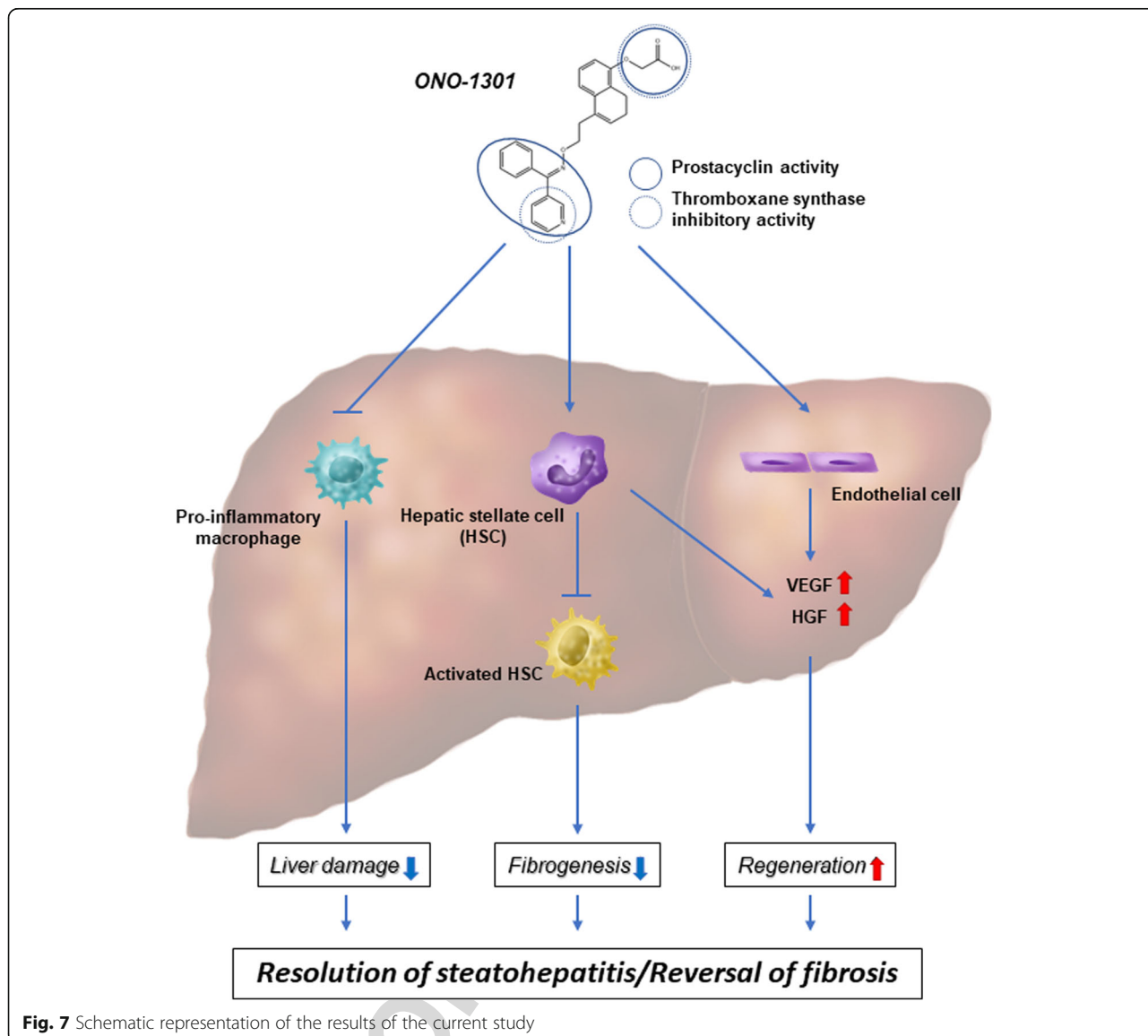
451 ONO-1301 (Fig. 6b). These results revealed that ONO-
 452 1301 affected HUVECs as an IP agonist.

453 **Discussion**

454 In this study, we demonstrated that ONO-1301 can
 455 ameliorate liver damage and fibrosis in a *Mc4r*-KO
 456 NASH mouse model. ONO-1301 had therapeutic effects
 457 regardless of the status of NASH and suppressed the oc-
 458 currence of liver tumors. ONO-1301 had multidirectional
 459 effects; ONO-1301 suppressed the inflammatory res-
 460 sponses of macrophages and activation of HSCs; it in-
 461 duced the production of VEGF from HSCs and that of
 462 HGF and VEGF from endothelial cells. Based on these re-
 463 sults, we concluded that ONO-1301 induces positive ef-
 464 fects on tissue repair in the NASH model mouse (Fig. 7). **F7**
 465 Originally, ONO-1301 was developed as an anti-
 466 platelet drug; however, a phase I clinical study showed
 467 adverse effects such as diarrhea and headache [18].
 468 Nevertheless, alternative medical effects of ONO-1301
 469 as a cytokine inducer or regeneration inducer were later
 470 identified using reduced doses in vitro. Thus, ONO-



f6.1
 f6.2
 f6.3
 f6.4



f7.1
f7.2

Fig. 7 Schematic representation of the results of the current study

471 1301 affects the IP receptors expressed in a variety of
 472 cells such as fibroblasts, vascular smooth muscle cells,
 473 and endothelial cells and upregulates the production of
 474 multiple factors, such as VEGF, HGF, and SDF-1, in-
 475 volved in tissue repair [14]. To date, the therapeutic ef-
 476 fects of ONO-1301 have been reported in a variety of
 477 diseases, such as pulmonary hypertension, pulmonary fi-
 478 brosis, arterial vascular disease, cardiac infarction [11,
 479 18], and obstructive nephropathy [13]. Thus, this drug is
 480 expected to be used for tissue repair in a variety of dis-
 481 eases and organs.

482 There are also some reports based on which we con-
 483 clude that ONO-1301 has positive effects in NASH.
 484 Some studies have reported that COX2 is upregulated in
 485 murine and human NASH livers [26–29], and Yu et al.
 486 reported that in a methionine- and choline-deficient diet

(MCDD)-induced NASH model mice, the hepatic ex- 487
 488 pression level of COX-2 was 10-fold higher than that in
 489 control mice [27]. Kumei et al., using IP-KO mice and a
 490 specific IP agonist and MCDD NASH model mouse, showed
 491 that PGI₂-IP signaling plays a crucial role in the develop-
 492 ment and progression of steatohepatitis by modulating the
 493 inflammatory response, leading to augmented oxidative stress
 494 [30]. Furthermore, Henkel et al. reported that attenua-
 495 tion of PGE₂ production by microsomal PGE synthase 1
 496 ablation enhances the THF- α -triggered inflammatory re-
 497 sponse and hepatocyte apoptosis in diet-induced NASH
 498 [31]. These reports suggest that ONO-1301, a synthetic
 499 prostacyclin IP receptor agonist that can induce endogenous
 500 PGI₂ and PGE₂, would be effective for NASH. Indeed, in
 501 our study, using the *Mc4r*-KO NASH model mouse, ONO-1301
 502

503 ameliorated liver damage and fibrosis by affecting mac-
 504 rophages, HSCs, and endothelial cells. Macrophages and
 505 HSCs are key players in liver inflammation and fibrosis;
 506 hence, we further investigated the effect of ONO-1301
 507 on these cells.

508 Regarding the effect of macrophages, Tsai et al. reported
 509 that PGI₂ analogs suppressed LPS-induced MIP-1 α pro-
 510 duction in human monocytes via the IP receptor and
 511 cAMP pathway. In this study, it was confirmed that
 512 ONO-1301 had a similar effect [32]. Pan et al. reported
 513 that forced expression of prostacyclin (PGI₂) synthase
 514 (PTGIS), which catalyzes the conversion of prostaglandin
 515 H₂ (PGH₂) to PGI₂, inhibits the macrophage switch to
 516 the M1 phenotype (pro-inflammatory macrophages), and
 517 promotes M2 polarization (anti-inflammatory macro-
 518 phages) [33]. Furthermore, PGE₂ is known to affect mac-
 519 rophages by inhibiting TNF- α and other macrophage-
 520 derived chemokines [31]. Kumei et al. reported that PGI₂
 521 analog Beraprost inhibited the LPS-induced activation of
 522 macrophages and improved the pathological condition of
 523 NASH [30]. These results are consistent with our results
 524 that ONO-1301 suppressed LPS-induced inflammatory
 525 responses in cultured macrophages.

526 Regarding HSCs, Mallat et al. reported that an increase
 527 in cAMP induced by PGI₂ and PGE₂ is related to the
 528 limited proliferation of activated HSCs during chronic
 529 liver damage [34]. Pan et al. reported that PTGIS in-
 530 hibits the activation of HSCs and alleviates liver fibrosis
 531 [35]. These results are consistent with our results show-
 532 ing that ONO-1301 suppressed HSC activation. Based
 533 on a previous study, we suspected that PGI₂-IP signals
 534 are important for inhibiting HSC activation.

535 As shown above, the main function of ONO-1301 is
 536 that it acts as a prostacyclin receptor (IP) agonist and in-
 537 hibits TXA₂ synthase. It prevents development of toler-
 538 ance caused by repeated IP agonist administration.
 539 However, in vivo, studies have reported very interesting
 540 results. Steib et al., reported that TXA₂ released from
 541 activated Kupffer cells was related to portal pressure and
 542 inhibition of TXA₂ reduced portal pressure in rats [36].
 543 This indicates that ONO-1301 may contribute to pre-
 544 vention of liver diseases.

545 Recent studies have developed improvised and modi-
 546 fied drugs from ONO-1301. ONO-1301SR, which is a
 547 poly lactic-co-glycolic acid (PLGA)-polymerized from
 548 ONO-1301, was developed to achieve a slow-releasing
 549 system of agents into target tissue, and the beneficial ef-
 550 fects of ONO-1301SR were confirmed using various ani-
 551 mal models of heart failure [17]. Furthermore, ONO-
 552 1301 nanospheres (ONONS) were developed to improve
 553 targeted delivery of ONO-1301 and were used to effi-
 554 ciently treat pulmonary artery hypertension [18]. These
 555 modified drugs decreased previously detected adverse ef-
 556 fects in human clinical trials.

This current study has some limitations. Although the
 557 *Mc4r*-KO mouse model is an ideal animal model for
 558 NASH, it does not completely recapitulate the character-
 559 istics of NASH in humans and requires a prolonged time
 560 to mimic the conditions of human NASH. Furthermore,
 561 it is ideal to use the macrophages, HSCs, and sinusoidal
 562 endothelial cells from NASH livers. However, bone
 563 marrow-derived macrophages were used to evaluate the
 564 function of macrophages, HSCs from old wild-type fe-
 565 male mice were used to evaluate inactivated HSCs, and
 566 HUVECs were used to evaluate the function of endothe-
 567 lial cells. These cells are of wild type mouse or human
 568 origin and do not completely reflect the function of
 569 macrophages, HSCs, and sinusoidal endothelial cells in
 570 NASH livers.
 571

572 Conclusions

573 Our study highlights the potential of ONO-1301 against
 574 liver inflammation, fibrosis, and tumor formation in
 575 NASH. ONO-1301 also significantly altered the mRNA
 576 expression of factors involved in tissue repair, further
 577 demonstrating its potential against liver damage. In con-
 578 clusion, ONO-1301, which has multiple functions (anti-
 579 inflammatory, anti-fibrosis, and production of multiple
 580 factors), is an attractive drug for treating liver diseases,
 581 including NASH, which often accompanies heart, kid-
 582 ney, and lung diseases.

583 Abbreviations

584 NAFLD: Non-alcoholic fatty liver disease; NASH: Non-alcoholic steatohepatitis;
 585 PG: Prostaglandin; TX: Thromboxane; IP: Prostacyclin receptor;
 586 cAMP: Adenosine cyclic 3',5'-monophosphate; HSC: Hepatic stellate cell;
 587 VEGF: Vascular endothelial growth factor; HGF: Hepatocyte growth factor;
 588 SDF-1: Stromal cell derived factor-1; NO: Nitric oxide; WD: Western diet;
 589 DMSO: Dissolved in dimethyl sulfoxide; DMEM: Dulbecco's modified Eagle's
 590 medium; LPS: Lipopolysaccharide; RT-PCR: Real-time polymerase chain
 591 reaction; FBS: Fetal bovine serum; mRNA: Messenger RNA; *Il6*: Interleukin-6;
 592 *Tnfa*: Tumor necrosis factor alpha; *Mcp1*: Monocyte chemoattractant protein-1;
 593 *Inos*: Inducible nitric oxide synthase; *Ym1*: Chitinase 3-like 3; *Il10*: Interleukin-
 594 10; *Cd206*: Macrophage mannose receptor; *Acta2*: Alpha-smooth muscle
 595 actin; *Col1a1*: Type I collagen alpha 1; *Col3a1*: Type III collagen alpha 1;
 596 *Ctgb*: Cytogloblin; *Hhpg*: Hedgehog interacting protein; HUVEC: Human
 597 umbilical vein endothelial cell; hCLS: Hepatic crown-like structures;
 598 ALT: Alanine aminotransferase; AST: Aspartate transaminase; Bil: Total
 599 bilirubin; ALB: Albumin; TG: Total triglyceride; T-cho: Total cholesterol;
 600 ConA: Concanavalin A

601 Supplementary Information

602 The online version contains supplementary material available at <https://doi.org/10.1186/s41232-021-00191-6>.

603
 604
 605
 606
 607
 608
 609
 610
 611
 612
 613
 614
 615
 616

Acknowledgements

We thank Takao Tsuchida for his cooperation in the preparation of the pathological tissue.

Authors' contributions

S. Motegei and A.T. collected and analyzed the data and wrote the manuscript. T.I., S.T., M.K., K.N., S.N., M.O., and S.T. collected and analyzed the data. Y. Sakai interpreted the data. Y. Sakai, S. Miyagawa, Y. Sawa, and S.T.

617 supervised the manuscript. All authors reviewed the manuscript. All authors
618 read and approved the final manuscript.

619 Funding

620 This research received no specific grant from any funding agency in the
621 public, commercial, or not-for-profit sectors.

622 Availability of data and materials

623 All data needed to evaluate the conclusions in the paper are presented in
624 the paper and/or the Supplementary Materials. Additional data related to
625 this study are requested from the authors.

626 Declarations

627 Ethical approval

628 All animal experiments were conducted in compliance with institutional
629 regulations, and the study protocols were approved by the Institutional
630 Animal Care and Committee of Niigata University.

631 Consent for publication

632 N/A.

633 Competing interests

634 Y. Sakai is the CEO of Lind Pharma, Inc. Y. Sawa and S. Miyagawa are the
635 scientific advisers of Lind Pharma Inc. The ONO-1301 was provided by Lind
636 Pharma Inc.

637 Author details

638 ¹Division of Gastroenterology and Hepatology, Graduate School of Medical
639 and Dental Sciences, Niigata University, 1-757, Asahimachi-dori, Chuo-ku,
640 Niigata 951-8510, Japan. ²Department of Cardiovascular Surgery, Graduate
641 School of Medicine, Osaka University, 2-2 Yamadaoka Suita, Osaka 565-0871,
642 Japan.

643 Received: 23 August 2021 Accepted: 20 December 2021

644

645 References

- 646 1. Younossi ZM, Koenig AB, Abdelatif D, Fazel Y, Henry L, Wymer M. Global
647 epidemiology of nonalcoholic fatty liver disease-meta-analytic assessment
648 of prevalence, incidence, and outcomes. *Hepatology*. 2016;64(1):73–84.
649 <https://doi.org/10.1002/hep.28431>.
- 650 2. Terai S, Buchanan-Hughes A, Ng A, Lee IH, Hasegawa K. Comorbidities and
651 healthcare costs and resource use of patients with nonalcoholic fatty liver
652 disease (NAFLD) and nonalcoholic steatohepatitis (NASH) in the Japan
653 medical data vision database. *J Gastroenterol*. 2021;56(3):274–84.
654 <https://doi.org/10.1007/s00535-021-01759-2>.
- 655 3. Eguchi Y, Hyogo H, Ono M, Mizuta T, Ono N, Fujimoto K, et al. Prevalence
656 and associated metabolic factors of nonalcoholic fatty liver disease in the
657 general population from 2009 to 2010 in Japan: a multicenter large
658 retrospective study. *J Gastroenterol*. 2012;47(5):586–95. <https://doi.org/10.1007/s00535-012-0533-z>.
- 660 4. Vuppalanchi R, Noureddin M, Alkhoury N, Sanyal AJ. Therapeutic pipeline in
661 nonalcoholic steatohepatitis. *Nat Rev Gastroenterol Hepatol*. 2021;18(6):373–
662 92. <https://doi.org/10.1038/s41575-020-00408-y>.
- 663 5. Watanabe T, Tsuchiya A, Takeuchi S, Nojiri S, Yoshida T, Ogawa M, et al.
664 Development of a non-alcoholic steatohepatitis model with rapid
665 accumulation of fibrosis, and its treatment using mesenchymal stem cells
666 and their small extracellular vesicles. *Regen Ther*. 2020;14:252–61.
667 <https://doi.org/10.1016/j.reth.2020.03.012>.
- 668 6. Yoshida T, Tsuchiya A, Kumagai M, Takeuchi S, Nojiri S, Watanabe T, et al.
669 Blocking sphingosine 1-phosphate receptor 2 accelerates hepatocellular
670 carcinoma progression in a mouse model of NASH. *Biochem Biophys Res
671 Commun*. 2020;530(4):665–72. <https://doi.org/10.1016/j.bbrc.2020.07.099>.
- 672 7. Sato T, Tsuchiya A, Owaki T, Kumagai M, Motegi S, Iwasawa T, et al. Severe
673 steatosis and mild colitis are important for the early occurrence of
674 hepatocellular carcinoma. *Biochem Biophys Res Commun*. 2021;566:36–44.
675 <https://doi.org/10.1016/j.bbrc.2021.05.097>.
- 676 8. Itoh M, Suganami T, Nakagawa N, Tanaka M, Yamamoto Y, Kamei Y, et al.
677 Melanocortin 4 receptor-deficient mice as a novel mouse model of
nonalcoholic steatohepatitis. *Am J Pathol*. 2011;179(5):2454–63. <https://doi.org/10.1016/j.ajpath.2011.07.014>.
9. Itoh M, Kato H, Suganami T, Konuma K, Marumoto Y, Terai S, et al. Hepatic
crown-like structure: a unique histological feature in non-alcoholic
steatohepatitis in mice and humans. *PLoS One*. 2013;8(12):e82163. <https://doi.org/10.1371/journal.pone.0082163>.
10. Xu Q, Nakayama M, Suzuki Y, Sakai K, Nakamura T, Sakai Y, et al. Suppression
of acute hepatic injury by a synthetic prostacyclin agonist through
hepatocyte growth factor expression. *Am J Physiol Gastrointest Liver
Physiol*. 2012;302(4):G420–9. <https://doi.org/10.1152/ajpgi.00216.2011>.
11. Uchida T, Hazekawa M, Yoshida M, Matsumoto K, Sakai Y. Novel long-acting
prostacyclin agonist (ONO-1301) with an angiogenic effect: promoting
synthesis of hepatocyte growth factor and increasing cyclic AMP
concentration via IP-receptor signaling. *J Pharmacol Sci*. 2013;123(4):392–
401. <https://doi.org/10.1254/jphs.13073FP>.
12. Murakami S, Nagaya N, Itoh T, Kataoka M, Iwase T, Horio T, et al. Prostacyclin
agonist with thromboxane synthase inhibitory activity (ONO-1301)
attenuates bleomycin-induced pulmonary fibrosis in mice. *Am J Physiol
Lung Cell Mol Physiol*. 2006;290(1):L59–65. <https://doi.org/10.1152/ajplung.00042.2005>.
13. Nasu T, Kinomura M, Tanabe K, Yamasaki H, Htay SL, Saito D, et al.
Sustained-release prostacyclin analog ONO-1301 ameliorates
tubulointerstitial alterations in a mouse obstructive nephropathy model. *Am
J Physiol Renal Physiol*. 2012;302(12):F1616–29. <https://doi.org/10.1152/ajprenal.00538.2011>.
14. Fukushima S, Miyagawa S, Sakai Y, Sawa Y. A sustained-release drug-delivery
system of synthetic prostacyclin agonist, ONO-1301SR: a new reagent to
enhance cardiac tissue salvage and/or regeneration in the damaged heart.
Heart Fail Rev. 2015;20(4):401–13. <https://doi.org/10.1007/s10741-015-9477-8>.
15. Obata H, Sakai Y, Ohnishi S, Takeshita S, Mori H, Kodama M, et al. Single
injection of a sustained-release prostacyclin analog improves pulmonary
hypertension in rats. *Am J Respir Crit Care Med*. 2008;177(2):195–201.
<https://doi.org/10.1164/rccm.200703-349OC>.
16. Li K, Zhao J, Wang M, Niu L, Wang Y, Li Y, et al. The Roles of Various
Prostaglandins in Fibrosis: A Review. *Biomolecules*. 2021;11(6):789. <https://doi.org/10.3390/biom11060789>.
17. Masada K, Miyagawa S, Sakai Y, Harada A, Kanaya T, Sawa Y. Synthetic
prostacyclin agonist attenuates pressure-overloaded cardiac fibrosis by
inhibiting FMT. *Mol Ther Methods Clin Dev*. 2020;19:210–9. <https://doi.org/10.1016/j.omtm.2020.09.005>.
18. Kanaya T, Miyagawa S, Kawamura T, Sakai Y, Masada K, Nawa N, et al.
Innovative therapeutic strategy using prostaglandin I2 agonist (ONO1301)
combined with nano drug delivery system for pulmonary arterial hypertension.
Sci Rep. 2021;11(1):7292. <https://doi.org/10.1038/s41598-021-86781-3>.
19. Kashiwagi H, Yuhki K, Kojima F, Kumei S, Takahata O, Sakai Y, et al. The
novel prostaglandin I2 mimetic ONO-1301 escapes desensitization in an
antiplatelet effect due to its inhibitory action on thromboxane A2 synthesis
in mice. *J Pharmacol Exp Ther*. 2015;353(2):269–78. <https://doi.org/10.1124/jpet.115.222612>.
20. Yin H, Cheng L, Langenbach R, Ju C. Prostaglandin I(2) and E(2) mediate the
protective effects of cyclooxygenase-2 in a mouse model of immune-
mediated liver injury. *Hepatology*. 2007;45(1):159–69. <https://doi.org/10.1002/hep.21493>.
21. Mayoral R, Molla B, Flores JM, Bosca L, Casado M, Martin-Sanz P. Constitutive
expression of cyclo-oxygenase 2 transgene in hepatocytes protects against
liver injury. *Biochem J*. 2008;416(3):337–46. <https://doi.org/10.1042/BJ20081224>.
22. Watanabe Y, Tsuchiya A, Seino S, Kawata Y, Kojima Y, Ikarashi S, et al.
Mesenchymal Stem Cells and Induced Bone Marrow-Derived Macrophages
Synergistically Improve Liver Fibrosis in Mice. *Stem Cells Transl Med*. 2019;
8(3):271–84. <https://doi.org/10.1002/sctm.18-0105>.
23. Takeuchi S, Tsuchiya A, Iwasawa T, Nojiri S, Watanabe T, Ogawa M, et al.
Small extracellular vesicles derived from interferon-gamma pre-conditioned
mesenchymal stromal cells effectively treat liver fibrosis. *NPJ Regen Med*.
2021;6(1):19. <https://doi.org/10.1038/s41536-021-00132-4>.
24. Campana L, Esser H, Huch M, Forbes S. Liver regeneration and
inflammation: from fundamental science to clinical applications. *Nat Rev
Mol Cell Biol*. 2021;22(9):608–24. <https://doi.org/10.1038/s41580-021-00373-7>.
25. Terai S, Tsuchiya A. Status of and candidates for cell therapy in liver
cirrhosis: overcoming the “point of no return” in advanced liver cirrhosis. *J
Gastroenterol*. 2017;52(2):129–40. <https://doi.org/10.1007/s00535-016-1258-1>.

- 749 26. Giannitrapani L, Ingrao S, Soresi M, Florena AM, La Spada E, Sandonato L,
750 et al. Cyclooxygenase-2 expression in chronic liver diseases and
751 hepatocellular carcinoma: an immunohistochemical study. *Ann N Y Acad*
752 *Sci.* 2009;1155(1):293–9. <https://doi.org/10.1111/j.1749-6632.2009.03698.x>.
- 753 27. Yu J, Ip E, Dela Pena A, Hou JY, Sessa J, Pera N, et al. COX-2 induction in
754 mice with experimental nutritional steatohepatitis: Role as pro-inflammatory
755 mediator. *Hepatology.* 2006;43(4):826–36. <https://doi.org/10.1002/hep.21108>.
- 756 28. Leclercq IA, Farrell GC, Sempoux C, dela Pena A and Horsmans Y. Curcumin
757 inhibits NF-kappaB activation and reduces the severity of experimental
758 steatohepatitis in mice. *J Hepatol.* 2004;41(6):926–34. <https://doi.org/10.1016/j.jhep.2004.08.010>.
- 760 29. dela Pena A, Leclercq IA, Williams J, Farrell GC. NADPH oxidase is not an
761 essential mediator of oxidative stress or liver injury in murine MCD diet-
762 induced steatohepatitis. *J Hepatol.* 2007;46:304–13.
- 763 30. Kumei S, Yuhki KI, Kojima F, Kashiwagi H, Imamichi Y, Okumura T, et al.
764 Prostaglandin I2 suppresses the development of diet-induced nonalcoholic
765 steatohepatitis in mice. *FASEB J.* 2018;32(5):2354–65. <https://doi.org/10.1096/fj.201700590R>.
- 766 31. Henkel J, Coleman CD, Schraplau A, Johrens K, Weiss TS, Jonas W, et al.
767 Augmented liver inflammation in a microsomal prostaglandin E synthase 1
768 (mPGES-1)-deficient diet-induced mouse NASH model. *Sci Rep.* 2018;8(1):
769 16127. <https://doi.org/10.1038/s41598-018-34633-y>.
- 770 32. Tsai MK, Hsieh CC, Kuo HF, Lee MS, Huang MY, Kuo CH, et al. Effect of
771 prostaglandin I2 analogs on monocyte chemoattractant protein-1 in human
772 monocyte and macrophage. *Clin Exp Med.* 2015;15(3):245–53. <https://doi.org/10.1007/s10238-014-0304-7>.
- 773 33. Pan XY, Yang Y, Meng HW, Li HD, Chen X, Huang HM, et al. DNA
774 Methylation of PTGIS Enhances Hepatic Stellate Cells Activation and Liver
775 Fibrogenesis. *Front Pharmacol.* 2018;9:553. <https://doi.org/10.3389/fphar.2018.00553>.
- 776 34. Mallat A, Preaux AM, Serradeil-Le Gal C, Raufaste D, Gallois C, Brenner DA,
777 et al. Growth inhibitory properties of endothelin-1 in activated human
778 hepatic stellate cells: a cyclic adenosine monophosphate-mediated
779 pathway. Inhibition of both extracellular signal-regulated kinase and c-Jun
780 kinase and upregulation of endothelin B receptors. *J Clin Invest.* 1996;98(12):
781 2771–8. <https://doi.org/10.1172/JCI119103>.
- 782 35. Pan XY, Wang L, You HM, Cheng M, Yang Y, Huang C, et al. Alternative
783 activation of macrophages by prostacyclin synthase ameliorates alcohol
784 induced liver injury. *Lab Invest.* 2021;101(9):1210–24.
- 785 36. Steib CJ, Gerbes AL, Bystron M, Op den Winkel M, Hartl J, Roggel F, et al.
786 Kupffer cell activation in normal and fibrotic livers increases portal pressure
787 via thromboxane A(2). *J Hepatol.* 2007;47(2):228–38. <https://doi.org/10.1016/j.jhep.2007.03.019>.

792 Publisher's Note

793 Springer Nature remains neutral with regard to jurisdictional claims in
794 published maps and institutional affiliations.

Ready to submit your research? Choose BMC and benefit from:

- fast, convenient online submission
- thorough peer review by experienced researchers in your field
- rapid publication on acceptance
- support for research data, including large and complex data types
- gold Open Access which fosters wider collaboration and increased citations
- maximum visibility for your research: over 100M website views per year

At BMC, research is always in progress.

Learn more biomedcentral.com/submissions



Author Query Form

Journal: Inflammation and Regeneration

Title: A novel prostaglandin I₂ agonist, ONO-1301, attenuates liver inflammation and suppresses fibrosis in non-alcoholic steatohepatitis model mice

Authors: Satoko Motegi, Atsunori Tsuchiya, Takahiro Iwasawa, Takeki Sato, Masaru - Kumagai, Kazuki Natsui, Shunsuke Nojiri, Masahiro Ogawa, Suguru Takeuchi, Yosiki Sakai, Shigeru Miyagawa, Yoshiki Sawa, Shuji Terai

Article: 191

Dear Authors,

During production of your paper, the following queries arose. Please respond to these by annotating your proofs with the necessary changes/additions. If you intend to annotate your proof electronically, please refer to the E-annotation guidelines. We recommend that you provide additional clarification of answers to queries by entering your answers on the query sheet, in addition to the text mark-up.

Query No.	Query	Remark
Q1	Please check if the section headings are assigned to appropriate levels.	
Q2	Figure/Table/Additional File: Please check and confirm if all captions and citations of Figures, Additional Files and Tables have been captured correctly.	
Q3	As per standard instruction, the statement "All authors read and approved the final manuscript." is required in the "Authors' contributions" section. Please note that this was inserted at the end of the paragraph of the said section. Please check if appropriate.	